Nov 3rd, 12:00 AM

Test and Finite Element Analysis on Distortional Buckling of Cold-formed Thin-walled Steel Lipped Channel Columns

Xingyou Yao

Yanli Guo

Zhiguang Huang

Twentieth International Specialty Conference on Cold-Formed Steel Structures
St. Louis, Missouri, U.S.A., November 3 & 4, 2010

Test and Finite Element Analysis on Distortional Buckling of Cold-formed Thin-walled Steel Lipped Channel Columns

Xingyou YAO[1], Yanli GUO[2], Zhiguang HUANG[3]

Abstract

High-strength cold-formed thin-walled steel sections have been widely used in the recent several years. However, distortional buckling or interaction between it and local buckling can occur for high strength cold-formed thin-walled steel members. This paper describes a series of compression tests performed on lipped channel section columns with V-shape intermediate stiffener in the web and flanges fabricated from cold-formed high strength steel of thickness 0.48 and 0.6mm with nominal yield stress 550MPa. The lipped channel sections were tested to failure with both ends of the columns fixed. The test results of 16 specimens show that the local buckling usually appears before distortional buckling of the specimens and it makes the distortional buckling occur in advance. This interaction of local and distortional buckling may have the effect of reducing the stiffness and bearing capacity of the columns. The comparison on ultimate strength and buckling mode between test results and results of finite element analysis considering geometric and material nonlinear show that finite element method (FEM) can simulate the distortional buckling of cold-formed steel channel columns effectively. The calculative results using Direct Strength Method (DSM) of the North American Specification show that this design method couldn't consider the reverse effect of interaction between local and distortional buckling on ultimate strength. Direct Strength Method (DSM) considering interaction between local and distortional buckling should be developed.

[1] Doctoral candidates, Tongji University, Shanghai, China

[2]Lecturer, Guangdong Ocean University, Zhanjiang, China

[3] Doctoral Candidates,Xi'an University of Architecture and Technology, Xi'an, China

Introduction

High strength cold-formed thin-walled steel sections with nominal yield stress 550MPa have been widely used in low-rise and multi-story residential buildings and portal steel frame structures in developed countries, especially in Australia. High strength steel members usually have low ductility and thinner and more complicated sections (see Fig.1). So those high strength cold-formed thin-walled sections may undergo local, distortional and overall buckling or mixed buckling modes. Meanwhile, geometry of section, mode of distortional buckling, load type, end supported condition, and stiffeners all effect on the ultimate strength of distortional buckling of cold-formed steel members, the accurate prediction on the member strength of thin-walled cold-formed steel sections becomes more complex.

Research into the distortional buckling mode of thin-walled cold-formed open sections has attracted considerable attention in recent years since the first discussion by Hancock (1985), Lau and Hancock (1987, 1990) tested a range of channel and rack sections columns and proposed a set of design chart and curve. Kwon and Hancock((1992,2004,2009) conducted compression tests of high strength cold-formed channel columns, which showed a substantial post-distortional buckling strength, and proposed a distortional buckling strength equation for the columns considered the interaction of buckling modes. Meanwhile, the Direct Strength Method (DSM), a new design method considering interaction of local or distortional and overall buckling modes, was developed by Shafer and Pekoz (1998) and was studied further by Hancock et al.(2001). North American Specification Supplement 1(NAS2004) and Australian/New Zealand Standard for Cold-formed Steel Structures Standard (AS/NZS 4600:2005) recently adopted the Direct Strength Method as an alternative to the conventional Effective Width Method to predict the member strength. However, extensive research into the interaction between local and distortional buckling has not been conducted yet.

Test investigations

Test specimens

As shown in Fig.1, a lipped channel section which has a V shaped stiffener in each flange as well as in the web was selected as specimens' section in order to ensure distortional buckling occur. The nominal dimensions of h, b, and d are 110, 80, and 12mm respectively for all sections. Meanwhile, sections have four kind of length for two kinds of thickness of 0.48 and 0.6mm respectively, including 500, 1000, 1500 and 2000mm. the width (S_{w1},S_{w2}) and height(S_{d1},S_{d2}) of V-shape intermediate stiffener of web and flange are 20 and 10 mm. the radius of corner(r) is 0.48 and 0.6mm for

columns of two different thickness. The nominal section geometric properties are shown in table 1.

Specimen labeling

The test specimens were labeled such that the type section, the nominal length and thickness of specimen and specimen number were expressed by the label. For example, the label “LCC2060-AC-2”defines the following specimen: 1. The first three letters indicate the specimen is a lipped channel section columns. 2. The “2060”indicate that nominal length and thickness of specimen is 2000 and 0.6mm. 3. The sequence number of same specimens was appended at the label end.

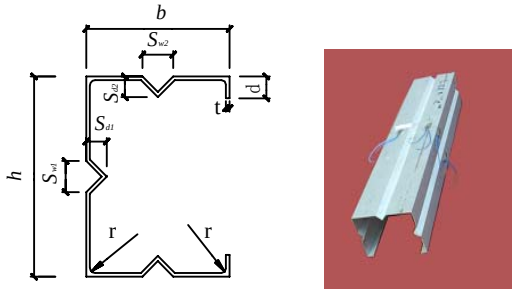

(a) Section dimensions （b）The specimen

Fig.1 Section of the specimens

Table 1 Nominal section properties of columns

specimen	*t*/ mm	Width-thickness ratio			*L*/mm	Slenderness ratio		Half-wavelength/ mm
		web	flange	lip		Strong axis	Weak axis	
LCC0548-1	0.48	229	167	25	500	10.9	17.4	1130
LCC0548-2	0.48	229	167	25	500	10.9	17.4	1130
LCC1048-1	0.48	229	167	25	1000	21.8	34.9	1130
LCC1048-2	0.48	229	167	25	1000	21.8	34.9	1130
LCC1548-1	0.48	229	167	25	1500	32.6	52.3	1130
LCC1548-2	0.48	229	167	25	1500	32.6	52.3	1130
LCC2048-1	0.48	229	167	25	2000	43.5	69.8	1130
LCC2048-2	0.48	229	167	25	2000	43.5	69.8	1130
LCC0560-1	0.60	183	133	20	500	10.9	17.4	995
LCC0560-2	0.60	183	133	20	500	10.9	17.4	995
LCC1060-1	0.60	183	133	20	1000	21.8	34.9	995
LCC1060-2	0.60	183	133	20	1000	21.8	34.9	995
LCC1560-1	0.60	183	133	20	1500	32.6	52.3	995
LCC1560-2	0.60	183	133	20	1500	32.6	52.3	995
LCC2060-1	0.60	183	133	20	2000	43.5	69.8	995
LCC2060-2	0.60	183	133	20	2000	43.5	69.8	995

Material properties

The structural steel grade of the test sections of thickness 0.48 and 0.60 mm was G550. The minimum specified yield stresses of the test sections of thickness 0.48 and 0.6mm is all 550MPa. Tensile coupons tested were

previously conducted for flat coupons cut from the fabricated sections. All coupons were tested in a 20kN capacity displacement controlled testing machine. The coupon test results were shown in table 2. The table 2 contains the experimental yield stress($f_{0.2}$), the ultimate stresses(f_u), and the initial Young's modulus(E). The experimental yield stress (2% offset) was higher than the nominal yield stress.

Test rig and gauge arrangement

Specimens were placed between the top and bottom end plates which is thick and flat enough to ensure fixed end boundary conditions. The 300kN capacity servo-controlled hydraulic testing machine system was used to apply compressive axial force for the specimens as shown in Fig.2. Load, strain, and displacement were recorded automatically by a date acquisition instrument and showed directly on the screen of the computer in this system. After geometric and physical alignment completed, axial loads can be subjected onto specimens by increments until the failure of them.

Table2 Material properties of columns

t/mm	*fu / MPa*	*f0.2/ MPa*	*E/ MPa*
0.48	727	695	216000
0.60	730	710	216000

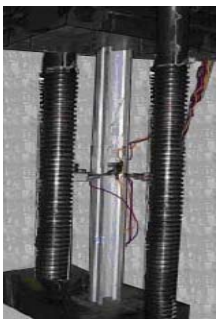

Fig.2 Set-up of the specimens

Lateral displacement transducers and strain gauges were commonly placed at mid-height of the columns, as shown in Fig.3 and Fig.4 for axially compressive specimens respectively. These strain gauges were used for alignment and to confirm buckling stress and experimental loading eccentricity.

Stud column test results

For shorter specimens of length 500mm, local buckling appeared first in the lip and then in the web (see Fig.5), distortion of flanges occurred nearly before the failure of specimens. These behaviors indicate that the failure of these shorter specimens resulted mainly from local buckling and significant distortional buckling only occurred when the ultimate load for local buckling was approached. Overall bucking wasn't obvious.

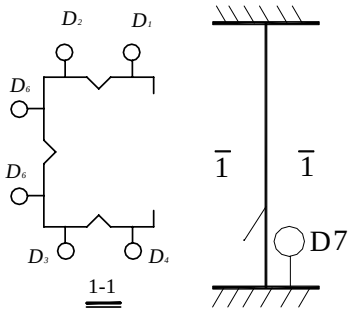

Fig.3 Displacement transducer

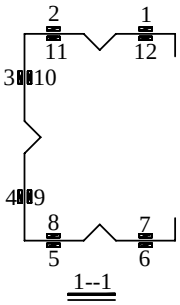

Fig.4 Strain gauges

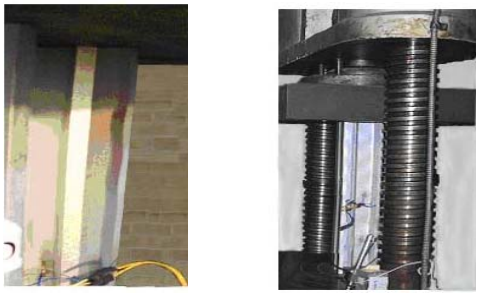

Fig. 5 Local buckling of stud column

Intermediate column test results

For specimens of intermediate lengths 1000mm and 1500mm, local buckling occurred in the web first and the obvious distortion of flanges occurred soon. The load of local buckling and distortional buckling was approximately same. Then the phenomena shows that local and distortional buckling almost existed simultaneously as shown in Fig.6. The member was failure with load and deflection increased. These specimens displayed a significant post-buckling strength reverse. These specimens were distortional buckling failure mode. Overall buckling wasn't obvious.

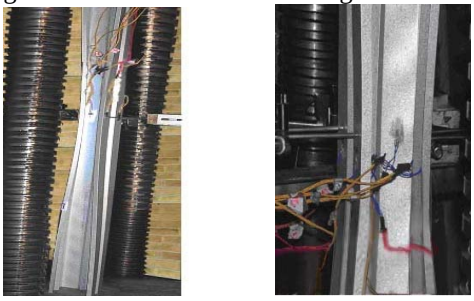

Fig.6 Buckling mode of medium-length specimens

Long column

For longer specimens of length 2000mm, the distortion of flanges appeared as soon as specimens were subjected to load as shown in Fig.7. With the load increasing, the distortional deformation of flanges got so significant that two flanges contact together. Local buckling in the web occurred nearly before the failure of specimen. These specimens were failure for large deflection of flange. So the main reason for the failure of longer specimens is distortional buckling. Interaction of local and distortional only occurred when the ultimate load was approached. Distortional buckling was obvious and the specimens occurred torsional-flexual deformation before the specimens were failure.

Fig.7 Buckling mode of longer specimens

Effect of buckling modes on ultimate load-carrying capacity

Three kinds of flange buckling mode shape were observed during tests. The specimens buckled inwards (I-I mode), outwards (O-O mode) for two flanges and one flange inward and one flange outward (I-O mode) respectively. The three buckling modes are shown in Fig.8.

(a) *I-I* mode (b)*O-O* mode (c) *O-I* mode

Fig.8 Three types of flange distortional buckling modes

The detailed reason is summarized as following: If the web (with intermediate stiffeners) occur local bucking firstly and local bucking deformed shape is symmetrical about inter-mediate stiffeners, I-I mode can occur; otherwise O-I mode can occur, O-O mode can occur if local buckling doesn't occur before distortional buckling occur. Test results

show that O-O mode bears the load highest, I-O mode takes second place, I-I mode is the lowest.

The test results show that the failure modes of all the specimens are distortional buckling. The ultimate load-carrying capacity and distortional buckling mode are shown in table 3.

Finite element analysis

The finite element method ANSYS8.1 considering the material non-linear and geometry large deformation was used to simulate the experimental behavior and ultimate strength of the compressive specimens. The FEM contain two stages. An eigenvalue elastic buckling analysis was performed to solve the probable buckling modes first, and then, the non-linear buckling analysis was carried out to predict the ultimate strength, deformation, and failure mode of the test specimens using arc-length method, which can follow the post-buckling range.

Element type and mesh

A four-node three-dimensional quadrilateral shell element with six degrees of freedom at each node was used in FEM. The elastic shell element, shell63, was used to obtain the critical elastic local buckling and distortional buckling mode and the assumed initial geometric imperfection shape, and the plastic shell element, shell181, was used in the non-linear analysis. The mesh element size of 10x10mm is best to simulate the behavior and ultimate strength of the specimens. The Finite element medal meshed is shown as Fig.9.

Boundary condition

The tested members were fixed at each end supported with plate, so the end plates were modeled in the FEM. All nodes of the top end are constrained on displacement in the X, Y-direction and rotation in all X, Y, and Z-direction, and the below end are constrained on displacement and rotation in all direction. In order to simulate the rigid loading plates, the CERIG command was used at both ends to create rigid regions. The loading point and reaction point were defined as the master nodes (see Fig. 10).

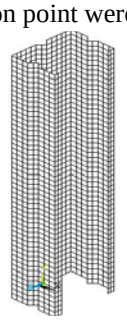

Fig.9 Finite element medal

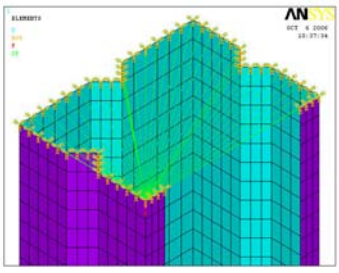

Fig. 10 Constrain on the reaction end

Geometric imperfection, material behavior

The geometric imperfection for the non-linear analysis was obtained by the eigenmode 1 multiplied a factor, which was specified by the maximum amplitude of the geometric imperfection measured for every specimen.

The material behavior was approximately described by a bilinear stress-strain curve, and the elastic modulus and the yield stress of the material were specified by the average of the material properties in Table1.

Failure mode and ultimate load prediction

The failure modes obtained from FEM were compared with the experimental failure modes as shown in Fig.11. Table3 summoned the ultimate strength analyzed by FEM. All results show that the failure mode and ultimate strength obtained from the FEM closed to the experimental failure modes and ultimate strength. So FEM can simulate the experimental buckling modes and calculate the ultimate loads closely.

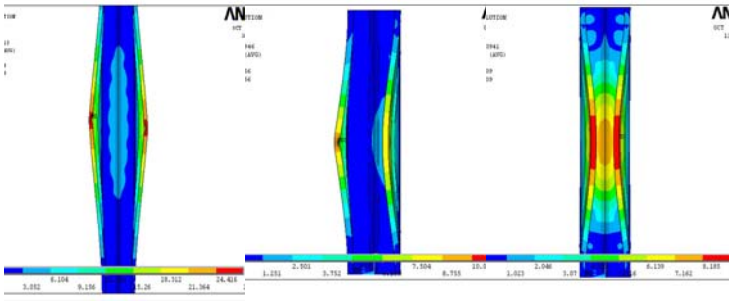

（a) *I-I* mode (b)*O-O* mode (c) *O-I* mode

Fig.11 distortional buckling modes of finite element analysis

Results compared with design methods

The supplement of North America Specification (NAS2004) provides the Direct Strength Method (DSM) to determinate the ultimate strength of axially compressive columns. The nominal member capacity of a member in compression shall be the minimum of the nominal member capacity of a member for flexural, torsional or flexural-torsional buckling, the nominal member capacity of a member in compression for local buckling and the nominal member capacity of a member in compression for distortional buckling. There are only the equations of the capacity for distortional buckling in this paper. These equations are

For $\lambda_d \le 0.561$ $\quad P_{nd} = P_y$ (1a)

For $\lambda_d > 0.561$ $\quad P_{nd} = P_y[1-0.25(P_{crd}/P_y)^{0.6}](P_{crd}/P_y)^{0.6}$ (1b)

Where $\lambda_d = \sqrt{P_y / P_{crd}}$; P_{crd} is the elastic distortional buckling strength; $P_{crd} = f_d \times A$; f_d is the elastic distortional bucking stress, which was obtained using the CUFSM, but the specimens all are fixed, so the elastic distortional buckling was obtained by the FEM; $P_y = AF_y$, A is the cross-sectional area, F_{y} is the yield strength.

The curve of member ultimate strength using Direct Strength Method (DSM) considering the minimum of the nominal member capacity of overall, local and distortional buckling against the length is shown in fig.11. Meanwhile, the average values of test results and the average values of finite element analytical results also are shown in fig.11. These results are also shown in table 3. As shown in table 3 and fig. 11, FEM can simulate the experimental buckling modes and calculate the ultimate loads closely. For the intermediate and long columns, the calculated results(P_{nd}) using NAS are higher than the test results(P_{t}), but the test results are close to the calculated results(P_{a}) using NAS for stud columns and long columns, because result from the intermediate columns display a significant interaction between local buckling and distortional buckling, which decrease the ultimate strength.

Table3 Comparison of experimental, FEA and NAS results

specimen	Test		Finite element method			North American specification	
	P_t/kN	buckling mode	P_a / kN	P_a/ P_{nd}	buckling mode	P_{nd} / kN	P_{nd}/ P_t
LCC0548-1	40.6	O-I	41.40	1.020	O-I	31.82	0.78
LCC0548-2	37.83	I-I	38.54	1.019	I-I	31.82	0.84
LCC1048-1	23.56	I-I	23.89	1.014	I-I	29.13	1.24
LCC1048-2	22.53	I-I	23.29	1.034	I-I	29.13	1.29
LCC1548-1	20.79	O-I	21.34	1.026	O-I	24.41	1.17
LCC1548-2	21.34	I-I	21.79	1.021	I-I	24.41	1.14
LCC2048-1	18.44	I-I	20.65	1.120	I-I	20.18	1.09
LCC2048-2	20.58	O-I	21.43	1.041	O-I	20.18	0.98
LCC0560-1	47.54	I-I	49.93	1.050	I-I	50.96	1.07
LCC0560-2	50.95	I-I	51.95	1.020	I-I	50.96	1.00
LCC1060-1	46.44	O-O	45.21	0.974	O-O	45.92	0.99
LCC1060-2	45.38	O-O	44.75	0.986	O-O	45.92	1.01
LCC1560-1	33.19	I-I	35.9	1.082	I-I	40.13	1.21
LCC1560-2	35.38	O-I	35.93	1.016	O-I	40.13	1.13
LCC2060-1	32.56	I-I	33.12	1.017	I-I	28.39	0.87
LCC2060-2	30.39	I-I	32.65	1.074	I-I	28.39	0.93

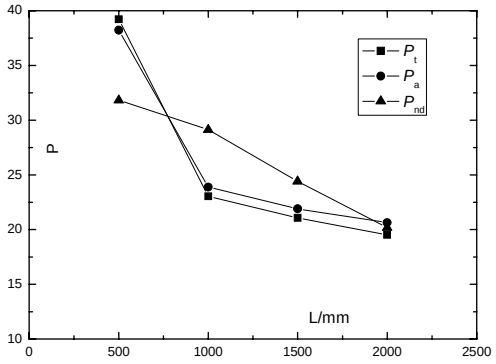

(a) t=0.48mm

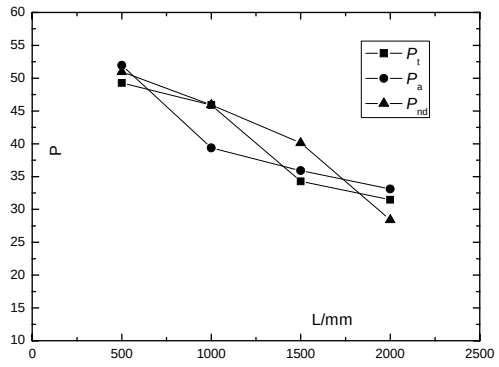

(b) t=0.6mm

Fig.10 flange distortional buckling modes of finite element analysis

Conclusion

The distortional buckling behavior of 16 high strength steel cold-formed thin-wall lipped channel specimens under axial compression loads have been tested in this paper. According to comparisons of test results and calculated results based on DSM and analytical results using FEM, the following conclusions can be drawn:

(1)Distortional buckling can occur in singly-symmetric sections of high strength cold-formed thin-walled steel columns if given certain section dimensions, and boundary conditions. Distortional buckling may control

member ultimate load-carrying capacity. So it should be considered in design.

(2)The behaviors of distortional buckling are much different from local or overall buckling of members. Therefore the design method for distortional buckling should be analysis.

(3)The stud columns display a significant post- local-buckling strength reverse and the distortional buckling just observe in the stage of failure, so the ultimate load-carrying capacity of the stud columns is relatively high. The intermediate and long columns display the distortional buckling early and interaction with local buckling which decrease the ultimate strength.

(4) FEM can simulate the experimental buckling modes and calculate the ultimate loads closely.

(5)The design formulas for the compressive column in DSM can be used to predict the ultimate strength for columns subjected to local and overall buckling, but can't be used to predict the ultimate strength for columns subjected to interaction between local and distortional buckling.

Notation

The following symbols are used in this paper:

A = cross-sectional area (mm^2);
b = flange width (mm);
d = lip width (mm);
E = initial Young's modulus (MPa);
$f_{0.2}$ = experimental yield stress (MPa);
f_d = elastic distortional bucking stress(MPa);
f_u = the ultimate stresses(MPa);
F_y = yield stress (MPa);
h = web height (mm);
L = length of column (mm);
P_a = FEM analytical ultimate strength (kN);
P_{crd} = elastic distortional buckling stength (kN);
P_{nd} = distortional buckling strength (kN);
P_t = ultimate test load (kN);
P_y = yield stength (kN);
R = the radius of corner(mm);
S_{w1},S_{w2} = width of V-shape intermediate stiffener of web and flange(mm);
S_{d1},S_{d2} = height of V-shape intermediate stiffener of web and flange (mm);
t = thickness of base metal (mm);

References

AS/NZS. (2005). “Cold-formed steel structures” *AS/NZS 4600: 2005*, Australian/New Zealand Standard, Sydney, Australia.

Hancock G. J. (1985), “Distortional buckling of steel storage rack columns”. *Journal of structural engineering*, 111(12):2770-2783.

Hancock G. J., Murray T.M. (2001), Cold-formed steel structures to the AISI specifications. Marcel Dekker, Inc..

Kwon Y.B., Kim B. S., Hancock G. J. (2009). “Compression tests of high strength cold-formed steel channels with buckling interaction”. *Journal of constructional steel research*. 65(2):278-289.

Kwon Y. B., Hancock G. J. (1992). “Test of cold-formed channels with local and distortional buckling”. *Journal of structural engineering*, 117(7):1786-1803.

Lau S.C.W., Hancock G. J. (1987), “Distortional buckling formulas for channel columns”. *Journal of structural engineering*, 113(5):1063-1078.

Lau S.C.W., Hancock G. J. (1990), “Inelastic buckling of channel columns in the distortional mode”. *Thin-Walled structures*, 10(2):59-84.

NAS.(2004). *Supplement 2004 to the North American specifications for the design of cold-formed steel structural members*, American Iron and Steel Institute, Washington D.C..

Schafer B. W., “Elastic buckling analysis of thin-walled members by finite strip analysis”, *CUFSM* v2.6.

Schafer B.W., Pekoz T. (1998) “Direct strength prediction of cold-formed steel members using numerical elastic buckling solutions”. In: Shanmugan NE, Liew JYR, Thevendran V, editors. *Thin-walled structures, research and development* Elsevier; 137-144.

Yang D.M., Hancock G. J.(2004). “Compression tests of high strength steel channel columns with interaction between local and distortional buckling”. *Journal of structural engineering*.2004, 130(12):1954-1963.